Magnetic and magneto-optical properties of NdX (X = P, As, Sb, Bi)

1999 J. Phys.: Condens. Matter 11 6277

(http://iopscience.iop.org/0953-8984/11/32/318)

J. Phys.: Condens. Matter **11** (1999) 6277–6286. Printed in the UK PII: S0953-8984(99)00247-7

Magnetic and magneto-optical properties of NdX (X = P, As, Sb, Bi)

Molly De and S K De

Department of Materials Science, Indian Association for the Cultivation of Science, Calcutta-700 032, India

Received 21 December 1998, in final form 17 May 1999

Abstract. The magnetic and magneto-optical properties of NdX (X = P, As, Sb, Bi) in the ferromagnetic phase derived from an electronic structure calculation have been presented. The calculation is performed using the local spin-density approximation (LSDA) and also the LSDA corrected with the Coulomb interaction U (the LSDA + U). The LSDA + U density of states at the Fermi level is small and the carrier density is also low. The magnetism in NdP, NdAs and NdSb is found to be dominated by a large orbital contribution coupled antiparallel to the spin moment. The anisotropic mixing between the p states of X and the f states of Nd provides the large off-diagonal optical conductivity.

1. Introduction

The magnetic properties of the cerium monopnictides CeX (X = P, As, Sb, Bi) are quite complex due to the anomalous behaviour of f electrons in Ce. Among the pnictides, CeSb has very unusual magnetic properties such as a large magnetic anisotropy with a small crystal-field splitting and an extremely complicated magnetic phase diagram [1–3]. The magnetic properties can be understood on the basis of hybridization between the f electrons and the non-f band electrons [4, 5]. The degree of localization, and hence the hybridization-induced exchange interaction, is very sensitive to the chemical environment and strongly dependent on the specific rare-earth element. The magnetic properties of NdX might prove to be interesting but have not yet been studied in detail.

The magneto-optical properties of certain light rare-earth compounds have caught the attention of physicists both from the theoretician's and the technologist's point of view. In recent years, the observation of the giant magneto-optical (MO) signals in some rare-earth compounds [6–8] has stimulated further studies carried out in order to gain an understanding of the microscopic origin of such a phenomenon. The MO properties are primarily dependent on the spin polarization and spin–orbit interaction. However, other electronic and magnetic properties such as orbital polarization, joint density of states (JDOS), oscillator strength and magnetic anisotropy are equally important for determining the magnitude of the MO signal. The recent studies of some Ce compounds indicate that the large MO signals are obtained for the compounds in which f electrons lie at the boundary between localized and delocalized behaviour [6]. The degree of delocalization of the f state is also an essential parameter governing the size of the MO signal. In fact Liechtenstein *et al* [9] have shown that anisotropy in the hybridization between the f bands of Ce and p bands of pnictogen together with a large spin–orbit splitting is responsible for that in CeSb. They have also found a better agreement of

0953-8984/99/326277+10$30.00

the off-diagonal conductivity using the LDA + U. On the other hand, Cooper *et al* [10] have held hybridization responsible for it, though the agreement with experiment is poor. Plasma frequency plays a crucial role for the large MO signals at low energy [11]. The exact mechanism for giant MO signals in some rare-earth compounds is not still clear. More experimental and theoretical studies are necessary to elucidate the origins of large MO signals.

The electronic and magnetic properties of NdX may be more interesting due to the dual (localized and delocalized) behaviour of f electrons. Previous experiments on magnetic and magneto-optical properties of Nd-based compounds are very few [12, 13]. The purpose of the present work is to investigate the electronic, magnetic and magneto-optical properties over a wide energy range of Nd monopnictides using electronic structure calculation. The electronic structure has been calculated using the linear muffin-tin-orbital (LMTO) method based upon local spin-density approximation (LSDA) and the Coulomb-corrected LSDA (the LSDA + U).

2. Method of calculation

Self-consistent band-structure calculations have been performed using the full-potential scalar relativistic linear muffin-tin orbital (LMTO) method [14] in the atomic sphere approximation (ASA). The non-spherical terms are taken into account in the charge density as well as in the potential. The ferromagnetic phase of NdX has been studied by spin-polarized electronic structure calculation in the framework of the local spin-density approximation. The spin–orbit interaction has been included in the Hamiltonian during the self-consistent calculations to investigate the orbital magnetism and magneto-optical spectra. Neodymium monopnictides, NdX, have NaCl structure and the lattice constant increases systematically from NdP to NdBi as shown in table 1. The Wigner–Seitz (WS) radii of the individual atoms are shown in table 1. The parametrization of the LSDA of von Barth and Hedin [15] has been used to construct the exchange–correlation potential. The density of states (DOS) has been calculated by the tetrahedron method [16].

Table 1. Input parameters for the band-structure calculation: a is the lattice constant; S(Nd) and S(X) are the Wigner–Seitz radii. All are in atomic units (au); 1 au = 0.529 Å.

NdX	a (au)	S(Nd) (au)	S(X) (au)
NdP	11.079	3.592	3.265
NdAs	11.259	3.650	3.318
NdSb	11.975	3.882	3.529
NdBi	12.149	3.939	3.581

The first-principles electronic calculation in the LSDA cannot predict many of the ground- and excited-state properties of the strongly correlated 4f systems. In order to account better for the on-site f-electron correlations, one should consider theories beyond the LSDA, such as that including a Hubbard term U in the LSDA (the LSDA + U). In this paper we have used the LSDA+U method to describe the ground-state electronic structure and the MO spectra of NdX. In the LSDA + U method, an orbital-dependent potential U acting mainly on localized f states is introduced in addition to the conventional LSDA potential. The total-energy functional in the LSDA + U scheme in terms of the Coulomb parameter U, the exchange parameter J and the total number of correlated electrons

$$N = \sum_{m,\sigma} n_{m,\sigma}$$

where $n_{m\sigma}$ is the occupancy of a particular $m\sigma$ orbital, is given by [17]

$$E_{\mathrm{LSDA}+U} = E_{\mathrm{LSDA}} - U\frac{N(N-1)}{2} - J\frac{N(N-2)}{4} + \frac{1}{2}\sum_{m,m',\sigma} U_{mm'}n_{m,\sigma}n_{m',-\sigma} + \frac{1}{2}\sum_{m\neq m',m',\sigma}(U_{mm'} - J_{mm'})n_{m,\sigma}n_{m',\sigma} \tag{1}$$

and the occupation-dependent one-electron potential is given by

$$V_{m\sigma}(r) = V_{LDA} + \sum_{m'}(U_{mm'} - J_{mm'})n_{m',-\sigma} + \sum_{m'\neq m}(U_{mm'} - J_{mm'} - U)n_{m,\sigma} + U\left(\frac{1}{2} - n_{m,\sigma}\right) - \frac{1}{4}J. \tag{2}$$

The Coulomb ($U_{mm'}$) and exchange ($J_{mm'}$) matrices are

$$U_{mm'} = \sum_k a_k F^k \tag{3a}$$

$$J_{mm'} = \sum_k b_k F^k \tag{3b}$$

$$a_k = \frac{4\pi}{2k+1}\sum_{q=-k}^{k}\langle lm|Y_{kq}|lm\rangle\langle lm'|Y^*_{kq}|lm'\rangle \tag{4a}$$

$$b_k = \frac{4\pi}{2k+1}\sum_{q=-k}^{k}|\langle lm|Y_{kq}|lm'\rangle|^2 \tag{4b}$$

where the F^k are Slater integrals and the $\langle lm|Y_{kq}|lm'\rangle$ are integrals over products of three spherical harmonics Y_{lm}. For f electrons, one needs the F^k ($k = 0, 2, 4, 6$) and these can be linked to the parameters U and J. The Coulomb parameter F^0 has been taken as 6.0 eV. For the other parameters, the values $F^k = 10.18, 6.39, 4.60$ eV (for $k = 2, 4, 6$) have been used, from the experimental x-ray absorption spectra [18].

The magneto-optical properties (MO), particularly the magneto-optic Kerr effect (MOKE), can be described by both diagonal and off-diagonal components of the conductivity tensor $\sigma_{\alpha\beta}$. The MO effect is determined by the spin–orbit interactions in the absence of the external magnetic field. The interband contribution to the absorptive part of the macroscopic conductivity tensor can be obtained from the following microscopic optical transitions:

$$\sigma_{xx}(\omega) = \frac{\overline{h}^2e^2}{12\pi^2m^2\omega}\sum_{i,f}\int_{\mathrm{BZ}}|\langle f|\boldsymbol{P}_x|i\rangle|^2\delta(E_f(\boldsymbol{k}) - E_i(\boldsymbol{k}) - \overline{h}\omega)\,\mathrm{d}\boldsymbol{k} \tag{5a}$$

$$\sigma_{xy}(\omega) = \frac{\overline{h}^2e^2}{12\pi^2m^2\omega}\sum_{f,i}\int_{\mathrm{BZ}}\mathrm{Im}(\langle f|\boldsymbol{P}_x|i\rangle\langle i|\boldsymbol{P}_y|f\rangle)\delta(E_f(\boldsymbol{k}) - E_i(\boldsymbol{k}) - \overline{h}\omega)\,\mathrm{d}\boldsymbol{k} \tag{5b}$$

where $\sigma_{xx}(\omega)$ and $\sigma_{xy}(\omega)$ are the real components of the diagonal and off-diagonal parts of the conductivity tensor $\sigma_{\alpha\beta}$, $\langle f|P_\alpha|i\rangle = -\mathrm{i}\overline{h}\langle f|\nabla_\alpha|i\rangle$ is the matrix element of the momentum operator, m and e are the mass and charge of the electron respectively, $\overline{h}\omega$ is the incident photon energy, $E_i(\boldsymbol{k})$ and $E_f(\boldsymbol{k})$ are the energies of the initial and final states and $\boldsymbol{k}$ is the wave vector inside the BZ where the transition $E_i(\boldsymbol{k}) \rightarrow E_f(\boldsymbol{k})$ occurs. The momentum matrix element has been determined as described by Hobbs *et al* [19]. The integration over the Brillouin zone has been carried out by the linear energy tetrahedron method [16].

3. Results and discussion

The LSDA partial density of states (DOS) of NdSb is shown in figure 1. The occupied part of the valence band consists of mostly Sb p states and some d and f states of Nd. The appearance of p, d and f states in the same energy region indicates that a significant hybridization occurs among them. The large narrow peak close to the Fermi level E_F is formed by Nd f states. The inclusion of spin–orbit coupling separates f bands into two groups, one below E_F and the other above E_F. The value of the DOS at E_F is very large: 474.59 states Ryd^{-1}. The conduction bands have mainly Nd d character.

The LSDA + U band structure of NdP is shown in figure 2 as an example. The entire energy band structure of NdX can be divided into three parts: below, around and above the

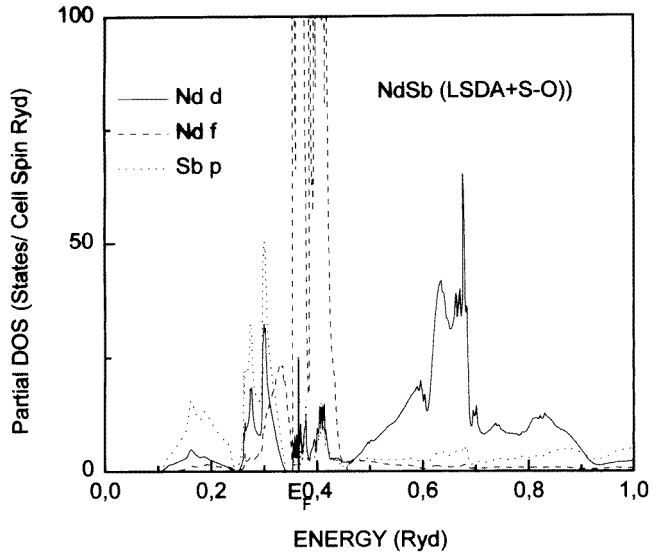

Figure 1. The partial density of states of NdSb.

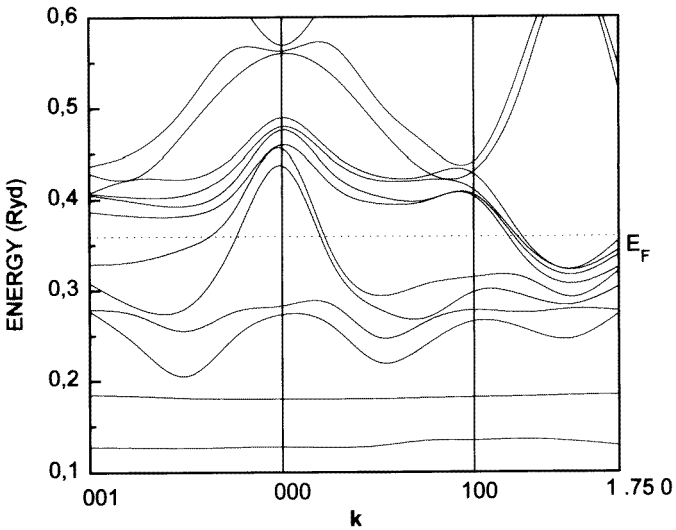

Figure 2. The electronic band structure of NdP.

Fermi level E_F. The nature, i.e. p, d and f character, of the bands can be understood from the angular-momentum-decomposed DOS, which is depicted in figure 3. The region well below E_F consists of two almost dispersionless bands in NdP as well as NdAs. These two bands, as is evident from figure 3, lie 0.2–0.3 Ryd below E_F and possess predominantly f character. The lowest singly occupied f band appears only slightly below E_F in contrast with the case for CeX [9]. The hybridization of these states with the X p states in this region is so insignificant that these bands appear dispersionless in figure 2. However, in NdSb, the two lowest bands are purely of f character and are far away from E_F. Figure 3 indicates that for the same energy position, the Nd f and Bi p states are strongly hybridized, thereby causing dispersion in the corresponding bands. This region is called the lower Hubbard band. The partial density of states in figure 3 shows that the states near E_F are p–d–f hybridized in NdP and NdAs and p–d hybridized in the heavier pnictides, NdSb and NdBi. The f states have narrow peaks below E_F and wide structures above E_F. The large splitting of the f states into the occupied and unoccupied f bands is obviously due to the strong on-site Coulomb repulsion effect on Nd f states. The unoccupied Nd f states along with the d states of Nd constitute the upper Hubbard band. The interesting feature noted is that there is a fair amount of anisotropy in the p–f mixing observed in all of the compounds NdX. In fact, the anisotropy in NdBi is such that some p bands are pushed above E_F along the Γ–Z axis but are partially occupied along the Γ–X axis. CeSb shows this kind of large anisotropy in the p–f mixing [9]. This suggests that there is a strong interaction between the p bands of X and the occupied Nd f bands. This anisotropy emerges from the symmetry-breaking nature of the LSDA + U approach. As one moves down the pnictide series, a remarkable difference is observed in the p states of X and f states of Nd. The characteristic trend in the electronic structure of the series arises due to the increasing influence of the spin–orbit splitting of the pnictogen p bands.

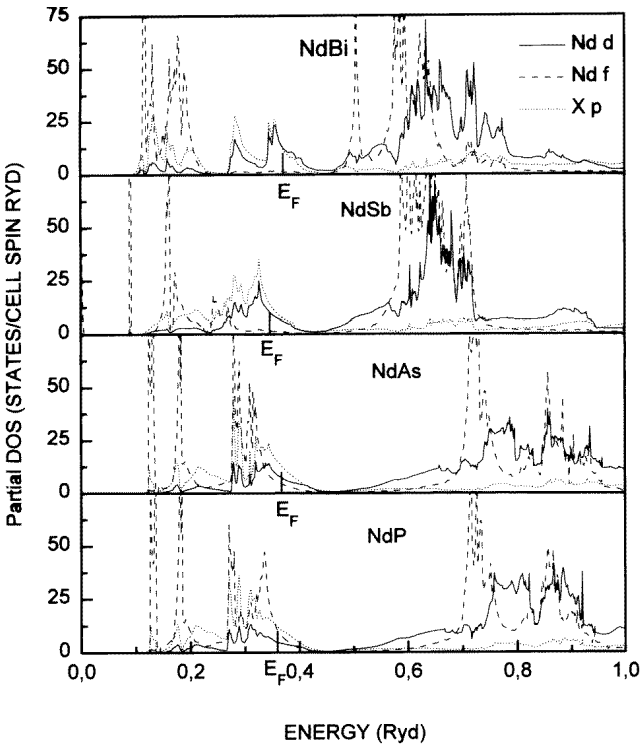

Figure 3. The partial density of states of NdX.

Table 2 contains the Fermi level, Fermi velocity, carrier concentration and plasma frequency for all of the pnictides. The low carrier concentration (∼3.5%) implies that the pnictides are all semi-metallic in nature, which was also found by Abdusalyanova *et al* [13]. In fact, this value is of the same order as for the compounds CeX [20–22], known to be low-carrier-density Kondo systems. The Fermi level lies in a region with a low density of states. The DOS at E_F obtained in NdSb is small as compared to the DOS (∼474.59 states Ryd^{-1}/cell) within LSDA (+spin–orbit) calculations. The usual large LSDA DOS at E_F due to the presence of the f bands is reduced to about 60 states Ryd^{-1}/cell. The angular-momentum-decomposed DOS at E_F for the pnictides reveals that the main contribution is from the Nd d states and X p states. The DOS due to the f states is small, reducing from 11.8 in NdP to 2.3 states Ryd^{-1}/cell in NdBi. This reduction in the DOS is due to the relativistic effects in the heavier pnictides. The rest of the contribution to the total DOS is from the Nd d states (about 20% in NdP to about 50% in NdBi) and X p states (about 50%). The greater availability of Nd d states at E_F implies greater p–d hybridization as the pnictogen size increases. At the Fermi level, p–f hybridization decreases, but it increases at the bottom of the valence band.

Table 2. Calculated values: the Fermi energy E_F, density of states $N(E_F)$, Fermi velocity v_F (one atomic unit of v_F is equal to 1.73×10^7 cm s^{-1}), carrier concentration n and plasma frequency ω_p.

NdX	E_F (Ryd)	$N(E_F)$ (states Ryd^{-1})	v_F (au)	n per formula unit	ω_p (eV)
NdP	0.359	60.52	2.33	0.034	8.63
NdAs	0.367	56.39	2.38	0.036	8.62
NdSb	0.346	57.18	2.39	0.036	7.89
NdBi	0.371	59.25	2.07	0.033	6.69

The spin, orbital and total magnetic moments are shown in table 3. The spin magnetic moment, m_s, is calculated by integrating the majority and minority components of the DOS up to E_F. The main contribution to m_s is from the f states of Nd and p states of X. The spin moments of Nd are larger compared to those of X for all of the pnictides. The Nd monopnictides are strongly spin polarized due to the high degree of spin splitting of the f states of Nd. The spin moments are of the same sign in Nd and X, i.e. the spins are aligned in the same direction in both. The total spin moments show a sharp decrease (they are almost halved) as one crosses over from NdAs to NdSb.

Table 3. Calculated spin (m_s) and orbital (m_o) magnetic moments (in μ_B) for NdX compounds.

	Nd		X		
NdX	m_s	m_o	m_s	m_o	M_{total}
NdP	3.62	−5.87	0.33	0.13	−1.79
NdAs	3.71	−5.89	0.39	0.14	−1.65
NdSb	1.86	−5.90	0.08	0.16	−3.80
NdBi	1.87	−0.06	0.11	−0.18	−1.74

The spin polarization and spin–orbit interaction produce the orbital moment. The orbital moment has been calculated from the orbital angular momentum density given by [23]

$$l_z(r) = \frac{1}{4\pi} \sum_{q,l,m,s} \int^{E_F} N_{qlms}(E) m \phi^2_{qls}(r, E)\, \mathrm{d}E \tag{6}$$

where s is the spin index, m is the azimuthal quantum number, N_{qlms} is the $qlms$-projected state density of the qth atom and the ϕ_{qls} are the corresponding atomic sphere wave functions.

The total moment is obtained in the ASA by integrating the moment density over the qth atomic sphere. The calculated orbital magnetic moments m_o of both Nd and X are summarized in table 3. It is clear that the Nd and X moments have a large and a quite small orbital component, respectively. The orbital contributions to the moment are larger than the spin contributions and also of opposite sign in all of the pnictides except NdBi. Nd has a less-than-half-filled 4f band; therefore the induced orbital moment is antiparallel to the 4f spin moment. The orbital polarization introduced by the LSDA + U method yields a greater orbital moment than the standard LSDA method. The total magnetic moment of NdSb is the largest among the compounds NdX. The magnetic properties of NdSb can be very interesting at low temperature. The total orbital moment is larger than that for the Ce monopnictides [9]. The hybridization of the Nd f states with Nd d and X p states affects the localization of the f electrons. Since the f states are pushed further below E_F, the hybridization of the f states with the X p states is smaller than that in CeSb. Hence the f electrons in Nd monopnictides are more localized. So, as the degree of localization increases, one finds that the lanthanides [6] show increasing orbital moment and decreasing exchange interaction.

The orbital polarization of NdBi differs quite considerably in magnitude at Nd sites and also in sign at X sites amongst the pnictides. The anomalous behaviour of the orbital magnetism in NdBi is certainly due to the greater p–f hybridization at the bottom of the valence band in NdBi. The lowest four bands of NdBi have significant Bi p contributions. This does not happen for the other pnictides, due to the smaller spin–orbit splitting of the pnictogen. Bismuth, being the heaviest, has the largest spin–orbit parameter [24]. The greater p–f hybridization has given rise to a sharp fall in the orbital moment, as has also been found by Wulff *et al* [25]. The alignment of the p orbitals of X is antiparallel to the total moment in all of the NdX compounds except NdBi. The orientation of the p orbitals of Bi in NdBi is opposite to that of the p orbitals of X in the other pnictides. The spin–orbit interaction in NdBi is such that the Bi p orbitals are oriented in the same direction as the Nd f orbitals.

The optical properties are usually calculated from the first-principles electronic energy band structure at zero temperature. As a result of this, the calculated spectra have many sharp peaks and a lot of fine structure, which can hardly be observed in experiments because of lifetime broadening effects, and also the instrumental resolution smears out many fine features. The intraband contribution to the conductivity is important at low energy and also in studying the lifetime broadening effects. The intraband effects on the diagonal part of the conductivity are obtained from the Drude expression

$$\sigma_{\alpha,\beta}^{intra} = \frac{\omega_{p,\alpha}^2 \tau}{4\pi(1 - \mathrm{i}\omega\tau)}\delta_{\alpha,\beta} \tag{7a}$$

where τ is the lifetime parameter and the plasma frequency ω_p^2 is given by

$$\omega_{p,\alpha}^2 = \frac{4\pi e^2}{V}\sum_n \sum_{k\in \mathrm{BZ}} \delta(E_{n,k} - E_F)(v_\alpha(n,k))^2 \qquad v_\alpha(n,k) = \frac{1}{\hbar}\frac{\partial E_{n.k}}{\partial k_\alpha}. \tag{7b}$$

The calculated values of the plasma frequency are shown in table 2. The plasma frequency is around 7–8 eV for the neodymium monopnictides, of the same order as but a little higher in magnitude than for the Ce chalcogenides [26].

The values of the diagonal optical conductivity σ_{xx} of NdX for the LSDA + U calculation are shown in figure 4. The calculated joint density of states (JDOS) excluding the momentum matrix elements in equation (5a) exhibits a small structure at very low energy (0.03 to 0.07 Ryd), another small structure at around 0.15 Ryd and a large peak at around 0.3 to 0.6 Ryd. The inclusion of the dipole matrix elements introduces restrictions on the probability of possible transitions in the JDOS imposed by the selection rules, $\Delta J = \pm 1$. The real part of the diagonal

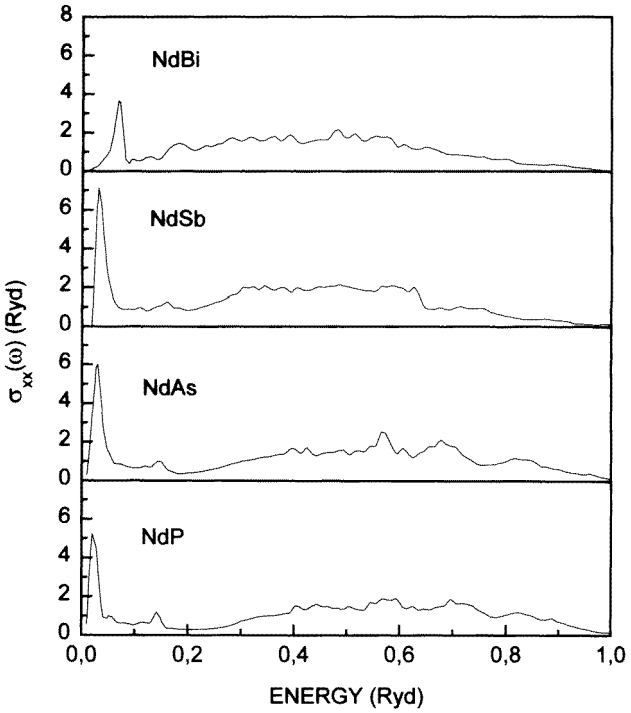

Figure 4. The real part of the diagonal conductivity of NdX.

conductivity, σ_{xx}, shown in figure 4, shows two main structures, one at very low energy and the other one at a much higher energy. The structure at around 0.15 Ryd loses its importance amidst the other two because p $\rightarrow$ p and p $\rightarrow$ f transitions are forbidden. The first peak shifts towards higher energy and becomes wider as the pnictide becomes heavier. This may be due to the effect of increasing spin–orbit coupling. The sharp peak at low energy (0.02–0.07 Ryd) is possibly due to p(X) $\rightarrow$ d(Nd) transitions and becomes more prominent due to the high p–d oscillator strength. This is so because the bands in the vicinity of E_F are p–d hybridized and the only transition possible is p $\rightarrow$ d. The transition occurs between the occupied and unoccupied parts of the p–d-hybridized bands. But the same spectrum for LSDA calculations does not exhibit such a prominent structure at such a small energy. A small structure at around 0.15 Ryd in this case may be attributed to d $\rightarrow$ f transition. The broad peak at around 0.4 Ryd is the result of f(Nd) $\rightarrow$ d(Nd) transitions in contrast to the p(X) $\rightarrow$ d(Nd) transitions in the LSDA calculation.

The real part of the off-diagonal conductivity, σ_{xy}, has been shown in figure 5 for the LSDA + U calculation. A strong peak at low energy is observed and raises the hope of getting some sort of magneto-optical signals. We cannot compare our results with experiments due to the non-availability of data, but it was observed that LSDA + U calculations provide good agreement with the experiments in the case of CeSb [9, 26]. From the partial DOS shown in figure 3, it is obvious that the negative peak at low energy comes from the p $\rightarrow$ d transition instead of the (p, f) $\rightarrow$ d transition for LSDA spectra. Moreover, in the LSDA calculations, this negative peak is substantially suppressed. The p bands involved in such transitions interact strongly with the occupied f bands of Nd anisotropically. The peak moves to higher energy and its height reduces as the pnictogen changes from P to Bi. The anisotropic p–f mixing leads to a splitting of the f character rather than to a dispersion of the f character over the valence band as

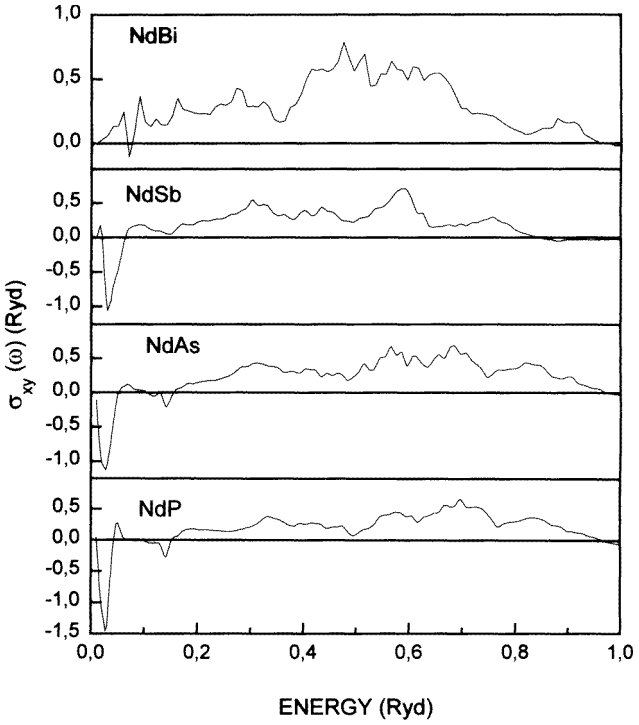

Figure 5. The real part of the off-diagonal conductivity of NdX.

occurs in the isotropic case. The behaviour of f states in the valence band indicates that the p–f mixing becomes more isotropic with the increase of the pnictogen atomic number. This effect may lead to the reduction in the off-diagonal optical conductivity. Larger values of σ_{xy} are obtained for the LSDA + U calculation compared with the LSDA treatment. This happens due to the differences in the nature of the p–f mixing in the two methods. The magnetic moment is mainly determined from the f states which are not involved in the transitions due to the removal of the f states from the region of E_F. The negative peak appears when there is strong orbital polarization [9, 10, 27, 28]. The weakest negative peak seen in NdBi may be due to the smallest orbital moment found among the NdX compounds. It is well known that the magneto-optical signals arise from a parity-breaking anisotropy in the motion of the electrons. In the absence of a magnetic field, this parity-breaking anisotropy results from spin–orbit interaction which couples the anisotropic spin in ferromagnets to the orbital motion. The considerable anisotropy in energy band structure and spin–orbit interaction among the electrons may be responsible for the negative peak in the low-energy region.

4. Conclusions

The electronic structure of the neodymium monopnictides in the ferromagnetic phase has been studied by the full-potential LMTO method within the LSDA + U and LSDA approximations, considering the spin–orbit coupling explicitly in the Hamiltonian. The introduction of the strong Coulomb correlation separates the f states into the upper and lower Hubbard bands, with the pnictogen p bands and Nd d bands occupying the region around the Fermi level. The p states of the pnictide ions play an important role in the electronic structure of NdX. All of them are semi-metallic in nature due to the low carrier density concentration. The large orbital

moment suggests that Nd f states are more localized than Ce f states. The small orbital moment of NdBi may be due to the strong spin–orbit interaction.

The magneto-optical properties and the magneto-optic Kerr effect are governed by the off-diagonal optical conductivity. A negative sharp peak is found for NdP, NdAs and NdSb at low energy in the off-diagonal conductivity spectra for both LSDA + U and LSDA calculations. The peak arises from f(Nd) $\rightarrow$ d(Nd) transitions and the f component is derived from the p–f mixed state by LSDA treatment. In the case of the LSDA + U calculation, p(X) $\rightarrow$ d(Nd) transitions give rise to this peak. The high orbital moment and the strongly anisotropic p–f mixing lead to large values of the off-diagonal conductivity. The larger values of the LSDA + U off-diagonal optical conductivity compared to the LSDA results indicate that for large Kerr rotation in NdX, strong on-site Coulomb correlation must be taken into consideration.

Acknowledgments

Molly De is grateful to the Council of Scientific and Industrial Research, Government of India, for financial support. The authors are grateful to Dr Sergej Savrasov for providing the FP-LMTO code. The authors are grateful to Professor S Chatterjee for his constant encouragement.

References

[1] Rossat-Mignod J, Effantin J M, Burlet P, Chattopadhyay T, Regnault L P, Bartholin H, Vettier C, Vogt O, Ravot D and Achart J 1985 *J. Magn. Magn. Mater.* **52** 111
[2] Chattopadhyay T, Burlet P, Rossat-Mignod J, Bartholin H, Vettier C and Vogt O 1994 *Phys. Rev.* B **49** 15 096
[3] Mori N, Okayama Y, Takahashi H, Haga Y and Suzuki T 1993 *Physica* B **186–188** 444
Mori N, Okayama Y, Takahashi H, Haga Y and Suzuki T 1993 *Physica* B **186–188** 531
[4] Wills J M and Cooper B R 1987 *Phys. Rev.* B **36** 3809
[5] Takahasi H and Kasuya T 1985 *J. Phys. C: Solid State Phys.* **18** 2695
[6] Pittini R and Wachter P 1998 *J. Magn. Magn. Mater.* **186** 306
[7] Pittini R, Schoenes J and Wachter P 1997 *Phys. Rev.* B **55** 7524
[8] Pittini R, Schoenes J, Vogt O and Wachter P 1996 *Phys. Rev. Lett.* **77** 944
[9] Liechtenstein A I, Antropov V P and Harmon B N 1994 *Phys. Rev.* B **49** 10 770
[10] Cooper B R, Lim S P, Avgin I, Sheng Q G and Price D L 1995 *J. Phys. Chem. Solids* **56** 1509
[11] Pustogowa U, Hubner W and Bennemann K H 1998 *Solid State Commun.* **106** 769
[12] Brandle H, Schoenes J and Hulliger F 1989 *Helv. Phys. Acta* **62** 199
[13] Abdusalyanova M N, Rakhmatov O I and Shokirov Kh Sh 1988 *Russ. Metall. (USA)* **1** 183
[14] Savrasov S and Savrasov D 1992 *Phys. Rev.* B **46** 12 181
[15] von Barth U and Hedin L 1972 *J. Phys. C: Solid State Phys.* **5** 1629
[16] Macdonald A H, Vosko S H and Coleridge P T 1979 *J. Phys. C: Solid State Phys.* **12** 2991
[17] Anisimov V I, Aryasetiawan F and Liechtenstein A I 1997 *J. Phys.: Condens. Matter* **9** 767
[18] Thole B T, van der Laan, Fuggle J C, Sawatzky G A, Karnatak R A and Esteva J M 1985 *Phys. Rev.* B **32** 5107
[19] Hobbs D, Piparo E, Girlanda R and Monaca M 1995 *J. Phys.: Condens. Matter.* **7** 2541
[20] Kwon Y S, Haga Y, Nakamura O, Suzuki T and Kasuya T 1990 *Physica* B **171** 324
[21] Kitzawa H, Oguru I, Hirai M, Kondo Y, Suzuki T and Kasuya T 1985 *J. Magn. Magn. Mater.* **47+48** 532
[22] Suzuki T 1993 *Physica* B **186–188** 347
[23] Brooks M S S and Cally P J 1983 *Phys. Rev. Lett.* **51** 1708
[24] Misemer D K 1988 *J. Magn. Magn. Mater.* **72** 267
[25] Wulff M, Eriksson O, Johansson B, Lebech B, Brooks M S S, Lander G H, Rebizant J, Spirlet J C and Brown P J 1990 *Europhys. Lett.* **11** 269
[26] Yaresko A N, Oppeneer P M, Antonov A Ya, Kraft V N and Eschrig H 1996 *Europhys. Lett.* **36** 551
[27] Lim S P and Copper B R 1991 *J. Appl. Phys.* **70** 5809
[28] Lim S P, Price D L and Cooper B R 1991 *IEEE Trans. Magn.* **27** 3648